On the origin and age of hydrothermal thorium-enriched carbonate veins and breccias in the Møre-Trøndelag Fault Zone, central Norway

A. GRØNLIE & T. H. TORSVIK

Grønlie, A. & Torsvik, T. H.: On the origin and age of hydrothermal thorium-enriched carbonate veins and breccias in the Møre-Trøndelag Fault Zone, central Norway. *Norsk Geologisk Tidsskrift*, Vol. 69, pp. 1–19. Oslo 1989. ISSN 0029–196X.

Fault-controlled, thorium-enriched carbonate veins of the inner Trondheimsfjord area have been investigated mineralogically and palaeomagnetically in order to provide a time-frame for tectonic and hydrothermal activity within the Møre–Trøndelag Fault Zone (MTFZ). As determined by optical microscopy, SEM and XRD, the red veins and breccias have a mineralogy dominated by quartz, K-feldspars, iron-carbonates, calcite, fluorite and barytes. The main thorium-containing phase is thorogummite $(Th(SiO_4)_{1-x}(OH)_{4x}$. The hydrothermal fluids which altered host-rocks adjacent to faults and joints changed throughout time. The earliest hydrothermal phase was one of Na-metasomatism, later followed by precipitation of iron-carbonates. Subsequent phases of hydrothermal alteration include a dominant phase of K-metasomatism and a later quartz, calcite and fluorite hydrothermal flux. Locally, veins and breccias are highly thorium-enriched, the average thorium content of analysed samples is 760 ppm, the Th/U-ratio being 28/1. The red veins disclose three remanence components, AI, AII and B, the first two being confined to highly radioactive, late-stage, thorium-enriched breccias. The B component is found both in host-rocks and hydrothermally altered veins. The results indicate magmatic and/or hydrothermal activity which we relate to tectonic events during Permian (B), Late Jurassic/Early Cretaceous (AII) and/or Late Cretaceous/Early Tertiary (AI) time.

A. Grønlie, Geological Survey of Norway, P.O. Box 3006-Lade, N–7002 Trondheim, Norway; T. H. Torsvik, Dept. of Earth Sciences, University of Oxford, OX1 3PR, U.K.

Nearly 700 red-coloured veins, alteration zones and breccias around the inner basin of Trondheimsfjord have been located during a project dealing with the evolution of the Møre–Trøndelag Fault Zone (MTFZ). Kjerulf (1875), working on the Ytterøy pyrite mine, was the first to describe these veins, or 'felsitganger', often resembling burnt rock.

The red veins cut metasediments, metavolcanics and igneous rocks in the nappes of the Middle and Upper Allochtons (Wolff 1976, 1984), and they are readily detected in the field due to their intense rusty- to brick-red coloration. The veins are often brecciated and crushed, and are characterized by high thorium contents. Thorium mostly occurs in thorogummite$(Th(SiO_4)_{1-x}(OH)_{4x})$, though the grainsize of this mineral is generally too small (5–20 μm) for detection in hand specimen. In the field, various carbonates such as ankerite-dolomite, calcite and siderite, together with quartz, K-feldspar, barytes and fluorite are readily observed. The red veins and breccia zones vary in width from 1 cm to more than 10 m, and some zones can be followed for several kilometres.

In our view, the majority of veins and breccias follow joints and faults initiated during a late event of extensional faulting. However, some of the more important breccias follow earlier fault trends apparently initiated during Late Devonian/Early Carboniferous collisional docking and strike-slip faulting within the MTFZ (Sturt et al. 1987; Torsvik et al. 1988a; Grønlie & Roberts 1987; Grønlie & Roberts 1989). It has also been proposed that the MTFZ later on was affected by Late Jurassic/Neocomian transpression, forming strike-slip duplex structures along the Verran Fault System (Fig. 1), as well as reactivating earlier faults (Grønlie & Roberts 1987; Larsen 1987).

Apart from a few igneous dykes and sills, no post-Silurian rocks occur onshore in this part of Norway. The timing of faulting and hydrothermal activity within the MTFZ thus cannot be estab-

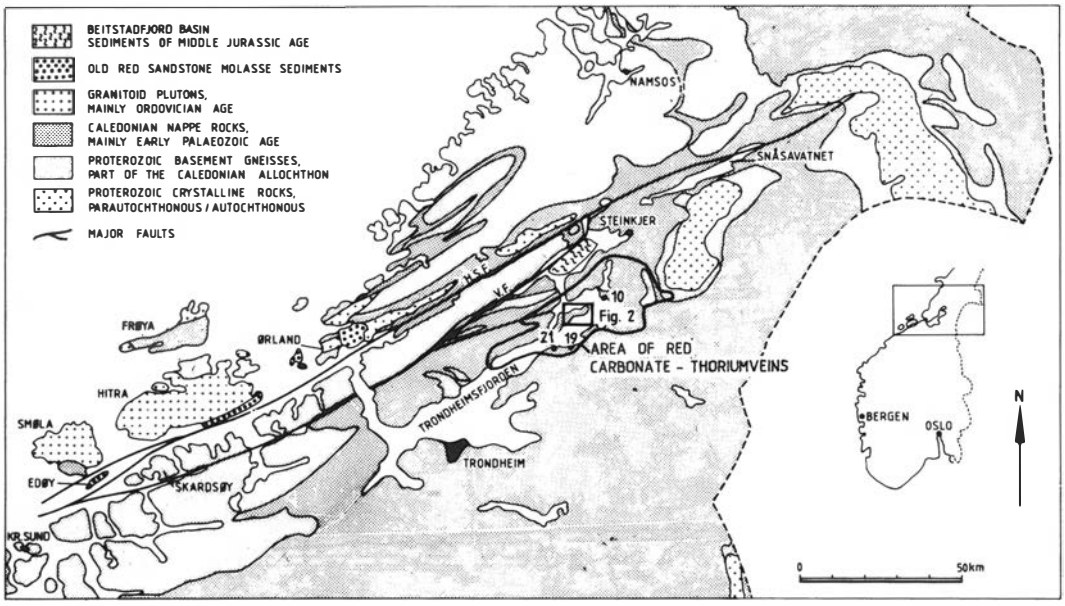

Fig. 1. Simplified outline geological map of the northern Trondheim Region showing the main tectonostratigraphic complexes and other rock units, and the principal strike-parallel faults. H.S.F. – Hitra–Snåsa Fault. V.F. – Verran Fault.

lished on a stratigraphic basis. A programme of palaeomagnetic (Sturt et al. 1987; Torsvik et al. 1988a) and radiometric dating of fault rocks has therefore been initiated. In the present account geochemical data are supplemented with palaeomagnetic data from fault rocks in order to provide a time-frame for faulting activity.

In this account the term thorium-enriched carbonate veins is employed as a common name for all hydrothermally altered veins and breccias, since iron-carbonates and thorium mineralization are widespread.

Description of red thorium-enriched carbonate veins

Most veins have been observed along the shoreline of the inner Trondheimsfjord basin (Fig. 1) (Staw 1986; Grønlie & Staw 1987). The island of Ytterøy (Fig. 2) is situated centrally in this zone of alteration, and appears to contain the greatest concentration of veins and breccias.

On the basis of field mapping, the following classification of the hydrothermal alteration phenomena can be made (Fig. 3):

(1) Single, thin red veins (Fig. 3a).

(2) Swarms of sometimes interconnecting red veins (Fig. 3b).

(3) Hydrothermally altered benches of host-rock (Fig. 3c).

(4) Major breccias, up to 10 m wide, generally containing abundant iron-carbonate and K-feldspar fragments. The surface is often covered by goethite (Fig. 3d).

(5) Highly radioactive quartz/K-feldspar/haematite/thorium-mineral rich breccia (referred to as thorium-enriched breccia or TE-breccia) (Figs. 3b, c, d).

A large number of minerals have been identified in the thorium veins (Table 1). Most of the veins and breccias contain quartz, microcline or adularia. Other common minerals are ankerite-dolomite, siderite, albite, calcite, apatite and fluorite. Microprobe analyses indicate that thorogummite ($Th(SiO_4)_{1-x}(OH)_{4x}$) and cheralite ($(Th,Ca,Ce)(PO_4,SiO_4)$) are the most common thorium minerals. They mostly occur as dusty, irregular, minute inclusions in K-feldspar. Monazite is commonly associated with, and shows the same mode of occurrence as, thorium minerals. As shown by microprobe analyses the ThO_2 content of thorogummite generally ranges from 48

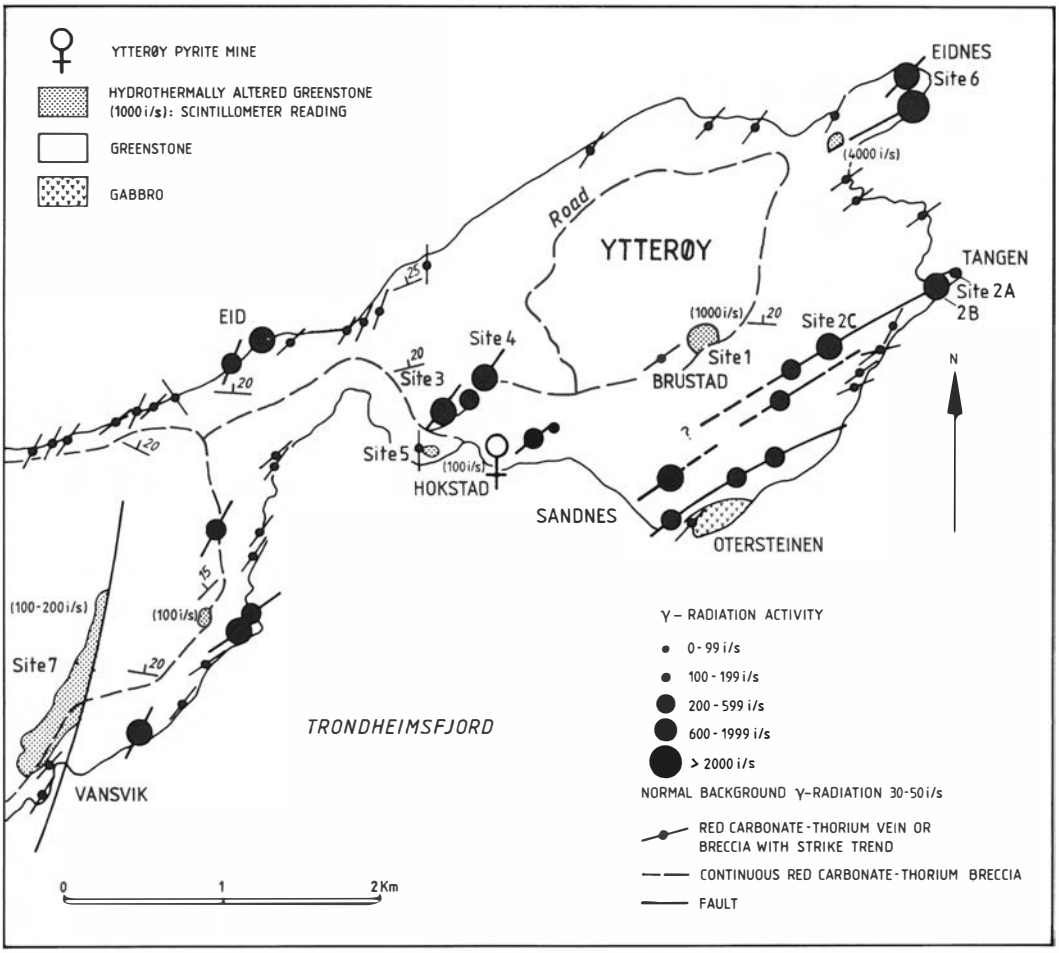

Fig. 2. Simplified geological map of parts of Ytterøy with occurrences of red carbonate-thorium veins and hydrothermally altered greenstones.

to 56%, while cheralite ranges from 25 to 27% (Grønlie 1984). A detailed analysis of the complicated mineralogy of thorium is beyond the scope of this paper and will be considered separately (Grønlie in prep.).

Alteration zones may occur as single, thin veins, and the alteration typically extends 1–10 cm on either side of a central joint. Joints often display a central fill of quartz, calcite or, more rarely, fluorite (Fig. 3a). The veins most commonly occur as swarms, and ca. 10–20 subparallel and sometimes interconnecting veins outcrop together in 1–5 m-wide zones (Fig. 3b). The alteration zones associated with individual veins may coalesce to leave the host-rock completely altered.

Although most red veins and alteration zones often appear homogeneous in the field, they are recurrently sheared and brecciated. A typical red alteration vein contains early quartz- and/or albite brecciated fragments exhibiting highly irregular, corroded outlines (Figs. 4a, b, c). Early brecciated quartz or albite was subsequently pervaded by fluids rich in Fe, Mg and CO_2, leading to precipitation of carbonates, mainly of the ankerite-dolomite series, but also modest amounts of siderite (Figs. 4a, c). Generally, this iron-carbonate phase was followed by a hydrothermal flux rich in potassium (Fig. 4d). K-feldspar, microcline or adularia (identified by XRD), is always dusted with inclusions of thorium-minerals and haematite (Figs. 5a, c), thus microcline never shows

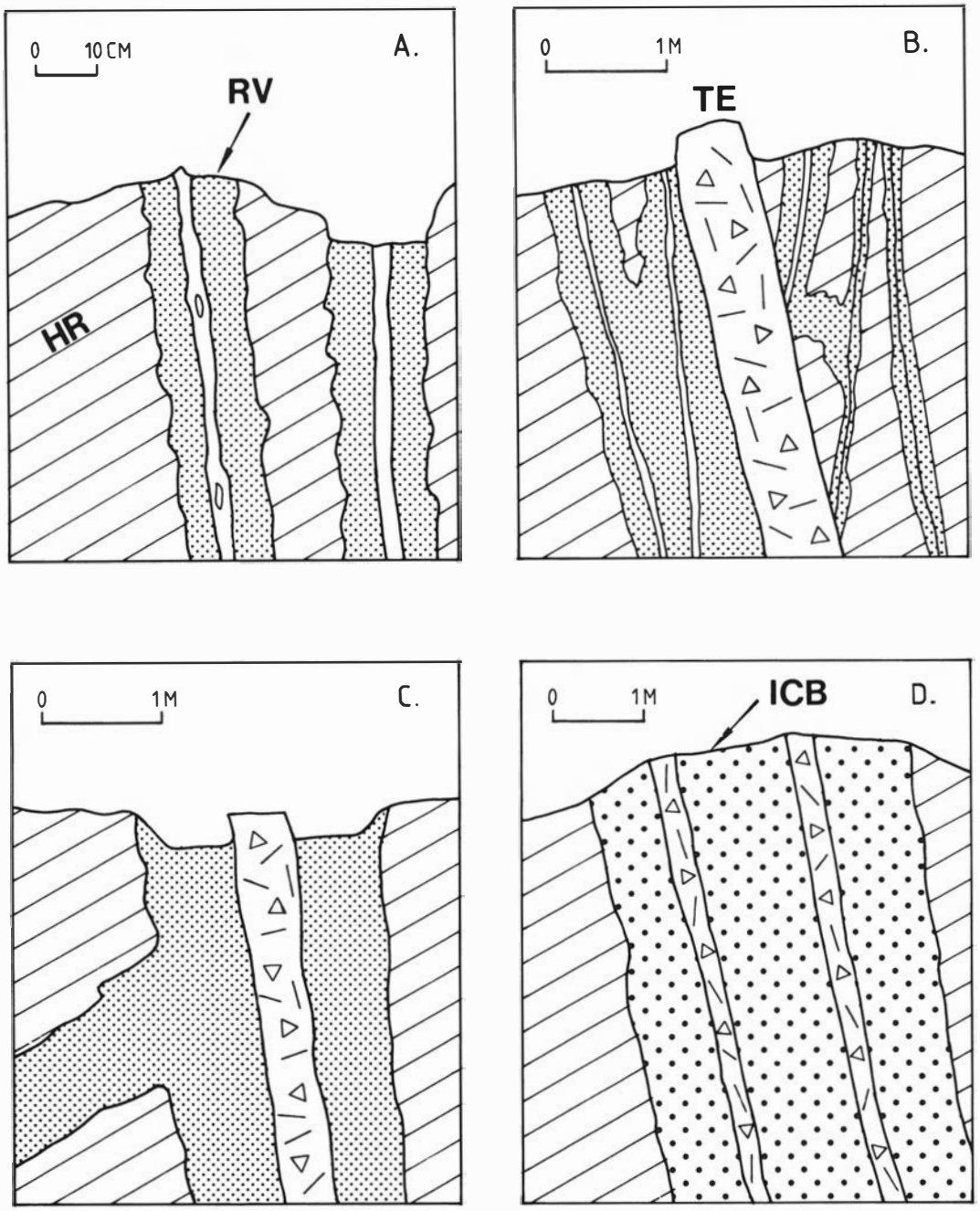

Fig. 3. (A) Single, red alteration veins. The red alteration zone in general consists of albite, ankerite-dolomite, siderite and K-feldspar with abundant enclosed haematite. The central, often drusy, vein fill, commonly consists of quartz (left), calcite (right) or, more rarely, fluorite. HR = host-rocks; RV = red alteration vein. (B) Swarm of subparallel and interconnecting red veins. Vein swarms are sometimes cut obliquely by a later, subparallel TE-breccia containing quartz, K-feldspar, haematite and thorium-minerals. The thorium-minerals, mostly thorogummite, occur as inclusions in K-feldspar or as discrete blebs and veinlets (cf. Fig. 5d). TE = thorium-enriched breccia. (C) Major red altered vein with hydrothermally altered host-rock parallel to layering. Alteration vein is later cut by TE-breccia. (D) Major breccia, generally containing abundant iron-carbonate, mostly ankerite-dolomite, as well as K-feldspar fragments. This carbonate-rich breccia is often transected by later TE-breccias. The major breccias are often intensely crushed and the surface covered by secondary goethite. ICB = iron-carbonate/K-feldspar fragment breccia.

Table 1. Minerals identified in red thorium-enriched carbonate veins.

Gangue minerals	
Quartz	SiO_2
Microcline	$(K,Na)AlSi_3O_8$
Adularia	$(K,Na)AlSi_3O_8$
Albite	$NaAlSi_3O_8$
Ankerite-dolomite	$CaMg_{1-x}Fe_x(CO_3)_2$
Siderite	$FeCO_3$
Calcite	$CaCO_3$
Barytes	$BaSO_4$
Apatite	$Ca_5(PO_4,CO_3OH)_3(F,Cl,OH,1/2O)$
Fluorite	CaF_2
Muscovite	$KAl_2Si_3AlO_{10}(OH)_2$
Iron-oxide minerals	
Goethite	$FeHO_2$
Haematite	Fe_2O_3
Magnetite	Fe_3O_4
Ilmenite	$FeTiO_3$
Thorium, Uranium and RE-minerals	
Thorogummite	$Th(SiO_4)_{1-x}(OH)_{4x}$
Cheralite	$(Th,Ca,Ce)(PO_4,SiO_4)$
Monazite	$CaPO_4$
Xenotime	YPO_4
Brannerite	$(U,Ca,Ce)(Ti,Fe)_2O_6$
Other minerals	
Rutile	TiO_2
Anatase	TiO_2
Zircon	$ZrSiO_4$
Sphene	$CaTiOSiO_4$
Pyrite	FeS_2
Chalcopyrite	$CuFeS_2$
Sphalerite	$(Zn,Fe)S$
Svanbergite	$SrAl_3(PO_4)(SO_4)(OH)_6$
Secondary clay minerals	—

cross-hatch twinning in thin-section. Late-stage mineralization of quartz, calcite and, more rarely, fluorite occurs as veins. The complete sequence of mineralizing events is not developed in all veins, since some veins apparently were aborted as fluid vents at some stage of the evolving hydrothermal system. Other veins and breccias are dominated by products of late-stage mineralizing fluids. An example of complete potassium-metasomatism occurs at Brustad, Ytterøy (site, 1, Fig. 2). At this locality the original greenstone and the earlier formed hydrothermal minerals were altered and adularite was developed. The adularite contains a few irregular apatite fragments as relics of the earliest hydrothermal phase (Fig. 5b, Table 2). Analyses of rocks from this site are almost identical with those of carbonatite related feldspathic fenitization products (Le Bas 1981).

Wide breccia zones, located to important faults and shear zones, in general contain the same minerals and paragenetic sequence as the thinner red veins. Due to several events of fault reactivation, however, they are often more complex and have a more heterogeneous fragment mineralogy. The bulk of such shear zones are often made up of a breccia consisting of 0.1 mm–2 cm angular ankerite-dolomite or siderite fragments in a matrix of K-feldspar or quartz. Fragments often comprise intergrowths of iron-carbonate and K-feldspar. More rarely, K-feldspar and iron-carbonate occur in a matrix of calcite. Quartz is the most common matrix mineral.

The radioactive part of breccias tend to be located in relatively narrow, 0.1–1 m wide, TE-breccias. Thorium-minerals and haematite occur

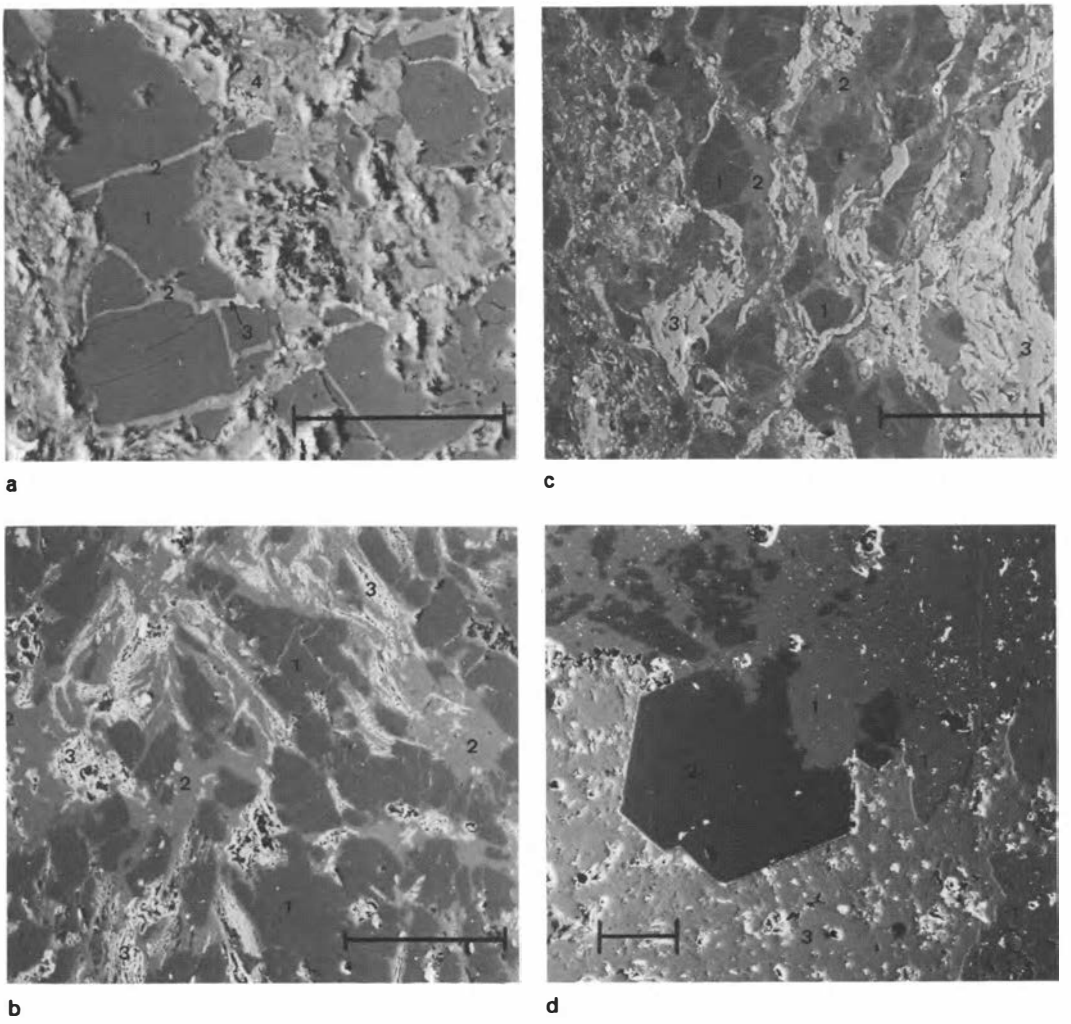

Fig. 4. (a) Early brecciated albite (1) veined by ankerite-dolomite (2) and siderite (3). Matrix mineral is partly clay-altered K-feldspar (4). Scale bar is 100 μm. Backscatter electron image. (b) Early brecciated and irregular albite (1) being replaced by K-feldspar phase (2) containing abundant haematite (3). Scale bar is 100 μm. Site 9, Ytterøy. Backscatter electron image. (c) Albite (1) being replaced by K-feldspar (2) and siderite (3). Thin, red alteration vein at site 12, Selbu, Børgin. Scale bar is 100 μm. Backscatter electron image. (d) K-feldspar (1) replacing quartz (2) and ankerite-dolomite (3). Carbonate-rich breccia near Ekne. Scale bar is 100 μm. Backscatter electron image.

together as discrete dark red veinlets or blebs (Fig. 5d) and disseminated, mostly in K-feldspar (Fig. 5a). The TE-breccias always formed later than the iron-carbonate hydrothermal phase.

On the basis of field observations, optical and electron microscopy a time sequence of the evolving hydrothermal system has been established. In general the following sequence of hydrothermal mineralization is observed (Fig. 6):

1. An early hydrothermal fluid phase led to replacement of the original host-rock by minerals such as quartz, albite and apatite.

2. This phase was followed by an Fe-, Mg- and CO_2 rich hydrothermal phase. This phase is characterized by replacement minerals with a composition near the ankerite end-member of the ankerite-dolomite series, as well as by siderite. Ankerite-dolomite and siderite can be observed either filling cracks in an early cataclastically deformed albite (Fig. 4a), or forming matrix min-

Table 2. Analyses (XRF) of red thorium-enriched carbonate veins.

	Site 1 Brustad Feldsp. fenite	Site 2b Tangen TE-breccia	Site 2c Tangen Carbonate-breccia	Site 10 Høsholmen Carbonate-breccia	Site 19 Sjøenget TE-breccia	Site 21 Ekne Feldsp. fenite	Brenne, Ytterøy. Greenstone
SiO_2	61.16	77.06	30.54	46.61	87.70	48.23	45.53
Al_2O_3	17.93	2.94	9.29	13.49	3.62	12.27	19.05
Fe_2O_3	2.37	0.44	1.15	0.59	0.41	2.78	11.91†
FeO	**	0.49	3.82	2.46	0.51	2.46	n.a.
TiO_2	0.37	0.04	0.43	0.35	0.07	0.77	0.89
MgO	<0.01	0.74	6.06	3.32	0.54	2.70	3.79
CaO	0.73	1.23	19.14	11.93	1.72	7.03	9.75
Na_2O	<0.1	<0.1	0.5	3.7	0.3	0.8	3.9
K_2O	14.98	1.84	7.31	5.45	2.50	9.93	0.29
MnO	0.09	0.01	0.17	0.11	0.02	0.10	0.16
P_2O_5	0.70	0.02	0.26	0.14	0.08	0.41	0.08
H_2O-	0.15	0.05	n.a.	n.a.	0.05	0.13	n.a.
H_2O+	0.39	0.03	n.a.	n.a.	0.09	0.25	n.a.
CO_2	0.08	2.12	n.a.	n.a.	2.48	11.62	n.a.
L.O.I.	—	—	19.01	9.66	—	—	3.75
Total	98.95	95.11	97.68	97.81	100.27	99.69	98.60
Nb	418	<5	<5	18	7	82	<5
Zr	34	90	<5	20	35	240	40
Y	17	24	31	43	19	91	20
Sr	782	0.15%*	643	617	137	473	511
Rb	345	45	157	131	62	227	7
Ba	549	7.72%*	565	262	519	356	28
U	<10	20	<10	10	<10	40	<10
Th	186	0.23%*	274	157	0.18%*	0.21%*	<10
Ce	80	154	14	<10	60	131	<10
La	29	38	<10	<10	23	53	<10

* Recalculated as oxides and included in total.

** Traces.

† Total iron as Fe_2O_3.

erals for partly replaced fragments of albite and quartz (Fig. 4c). The iron-carbonates are often intimately intergrown with K-feldspar, sometimes leaving doubt as to which mineral crystallized first (Fig. 4c). In cases where the crystallization sequence can be established without doubt, the iron-carbonates were the first precipitated minerals (Fig. 4d).

3. K-rich fluids leading to extensive potassium-metasomatism of the earlier vein material as well as the bordering host-rocks followed the crystallization of the iron-carbonate minerals. K-feldspars, either microcline or adularia, always contain abundant inclusions of haematite and thorium-minerals, mainly thorogummite (Fig. 5a). K-feldspar occurs in all veins and breccias, sometimes as the dominant mineral, and in extreme cases both breccia minerals and bordering host-rocks are pervasively affected by potassium-metasomatism.

4. Veins of quartz or calcite occur either filling central parts of joints associated with red veins or more irregularly. Quartz can be clear, milky white or, more rarely, smoky grey and is sometimes highly radioactive due to abundant inclusions of thorium-minerals. Late quartz sometimes replaces earlier formed K-feldspar dominated veins and breccias.

5. Blue fluorite occurs as a late matrix or vein material, often with thorium-mineral inclusions.

Chemical composition

A large number of red thorium-enriched carbonate veins have been analysed for major and

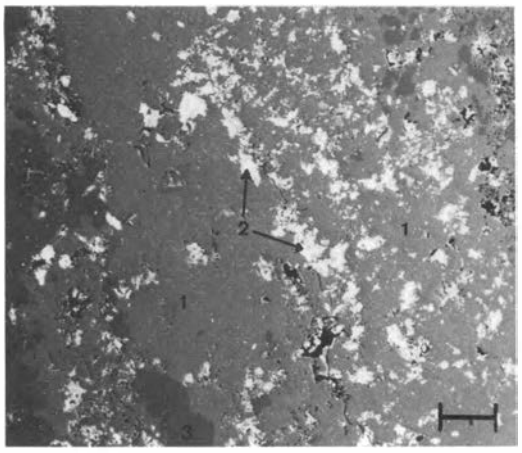

a

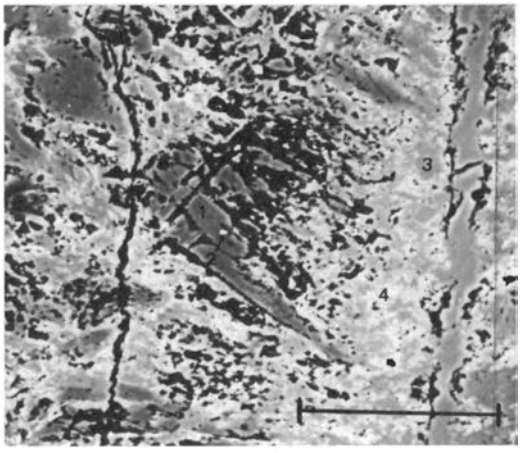

c

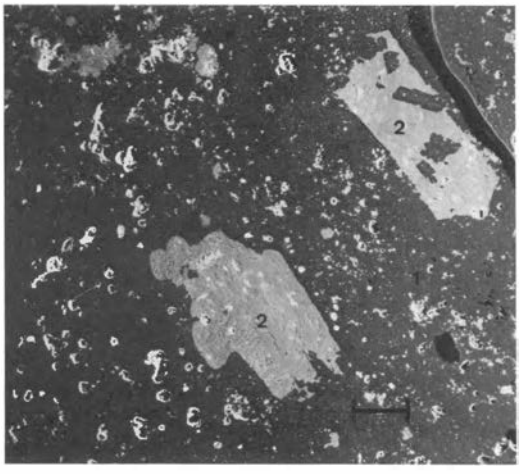

b

d

Fig. 5. (a) K-feldspar (1) containing abundant irregular thorogummite (2) replaces quartz (3). Site 25, Leks vik. Scale bar is 100 μm. Backscatter electron image. (b) Adularia (1) replacing apatite (2). The original greenstone host-rock has been altered to a feldspathic fenite consisting of nearly pure adularia (analysis, see Table 2). Site 1, Brustad, Ytterøy. Scale bar is 100 μm. Backscatter electron image. (c) Ankerite-dolomite (1) containing thorogummite (2) being replaced by K-feldspar (3) containing abundant haematite (4). Leks vik. Scale bar is 100 μm. Backscatter electron image. (d) Autoradiography of TE-breccia. Light blebs and veinlets correspond to thorium-mineral enrichment. (Ilford FP-4, 125ASA, exposed 14 days, contact print here reduced to half natural size).

trace elements (XRF). Representative analyses of the various alteration types (carbonate-dominated, feldspathic fenites and TE-breccias) are given in Table 2.

Major and trace elements were analysed on rock powders using an automatic Philips 1450/20 XRF, at the Section for Analytical Chemistry, NGU, Trondheim. Calibration curves were made with international standards. For the determination of major elements the rock samples were melted with lithium tetraborate 1/7. Trace elements were determined on pressed rock powder. Ferrous iron, H_2O+, H_2O- and CO_2 were determined by wet chemical methods.

The thorium content is erratically distributed within single veins, and shows large variations within each vein. Thorium in the sampled material (N = 84) averages 760 ppm, ranging from 10 ppm

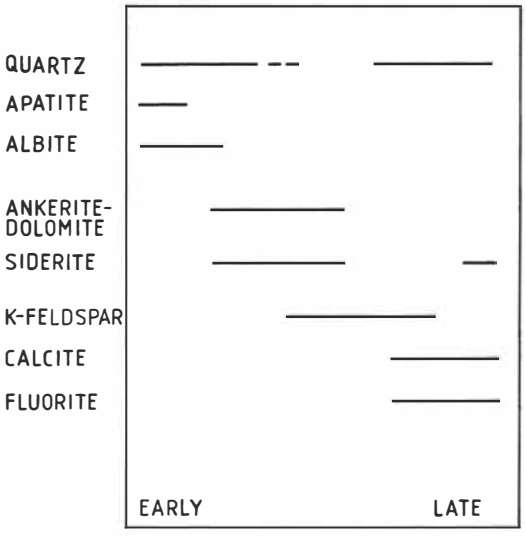

Fig. 6. Paragenetic sequence of minerals in the Trondheimsfjord red thorium-enriched carbonate vein system.

to 1.3%. The average Th/U ratio is 28/1. Iron-carbonate dominated samples usually contain thorium in the 100–500 ppm range, while feldspathic fenites and TE-breccias generally contain between 0.1% and 0.2% Th, although some samples contain more than 1% Th.

In this account only the rare-earth elements Ce and La plus Y have been analysed (XRF). No samples contain more Ce + La than Th, and the average Th/Ce + La + Y ratio is 5/1. Microprobe analysis of Th and RE minerals (Grønlie 1984) indicates that Nd occur in greater amounts than La in thorogummite, and equal amounts in monazite.

Spidergrams of chondrite-normalized incompatible elements of selected vein samples show that the common denominator for all samples is the high thorium-enrichment (Fig. 7), and a depletion in Ti, particularly in the TE-breccias. It must be borne in mind that the samples represent different types of veins and breccias, e.g. samples 1 and 21 are compositionally similar to feldspathic fenites (Le Bas 1981), while samples from sites 2c and 10 are carbonate-fluorite dominated veins. Site 2b and 19 are TE-breccias. Consequently, the spread of values for elements such as Nb is large. The feldspathic fenites of site 1 and 21 show the highest Nb and K enrichments whilst TE-breccias (site 2a and 19) show the lowest values.

Palaeomagnetic experiments

Eight sites (152 samples) were selected for palaeomagnetic purposes, and six sites embrace red thorium-enriched carbonate veins in the Ytterøy region. Additionally, two sites were sampled from breccias associated with the Hitra and Verran Fault Zones (Fig. 1).

The natural remanent magnetization (NRM) was measured on a two-axis cryogenic magnetometer, and progressive thermal demagnetization was applied for NRM stability testing. Characteristic remanence directions were calculated from least square analysis.

Hydrothermal breccias and altered host-rocks contain a variety of opaque minerals including haematite, magnetite, geothite and accessory pyrite, ilmenite and rutile (Table 1). Goethite is observed together with iron-carbonates (e.g. siderite) and K-feldspar, and is notably abundant where repeated brecciation and metasomatism has taken place. This may indicate that goethite was formed to a large extent by later alteration of iron-carbonates, but also through weathering of magnetite.

Host-rock samples are considerably more thermochemically stable than brecciated and hydrothermally altered samples, and isothermal remanent magnetization curves are normally dominated by variable proportions of a low-coercivity phase and a high-coercivity phase. These were identified, as magnetite and haematite respectively, by means of thermomagnetic analysis and inspection of the thermal blocking temperature spectra. Breccias often display large magnetomineralogical changes during heating, and remanence stability recurrently ceased at intermediate temperatures (350–450°C). This remanence instability, occasionally associated with increase in the NRM, presumably relates to one or a combination of the following processes:

1. Dehydration of goethite to form haematite.
2. Alteration of iron-bearing minerals to form magnetite.
3. Pyrite inverting to magnetite and/or pyrrhotite.

Goethite and pyrite are common minerals in all the tested breccias, and goethite occurs as a late-stage weathering product of magnetite, pyrite and iron-carbonates (mainly siderite), but could also have formed by direct precipitation from the early iron-carbonate enriched fluids, and partly dehydrated to haematite at a later stage. Goethite

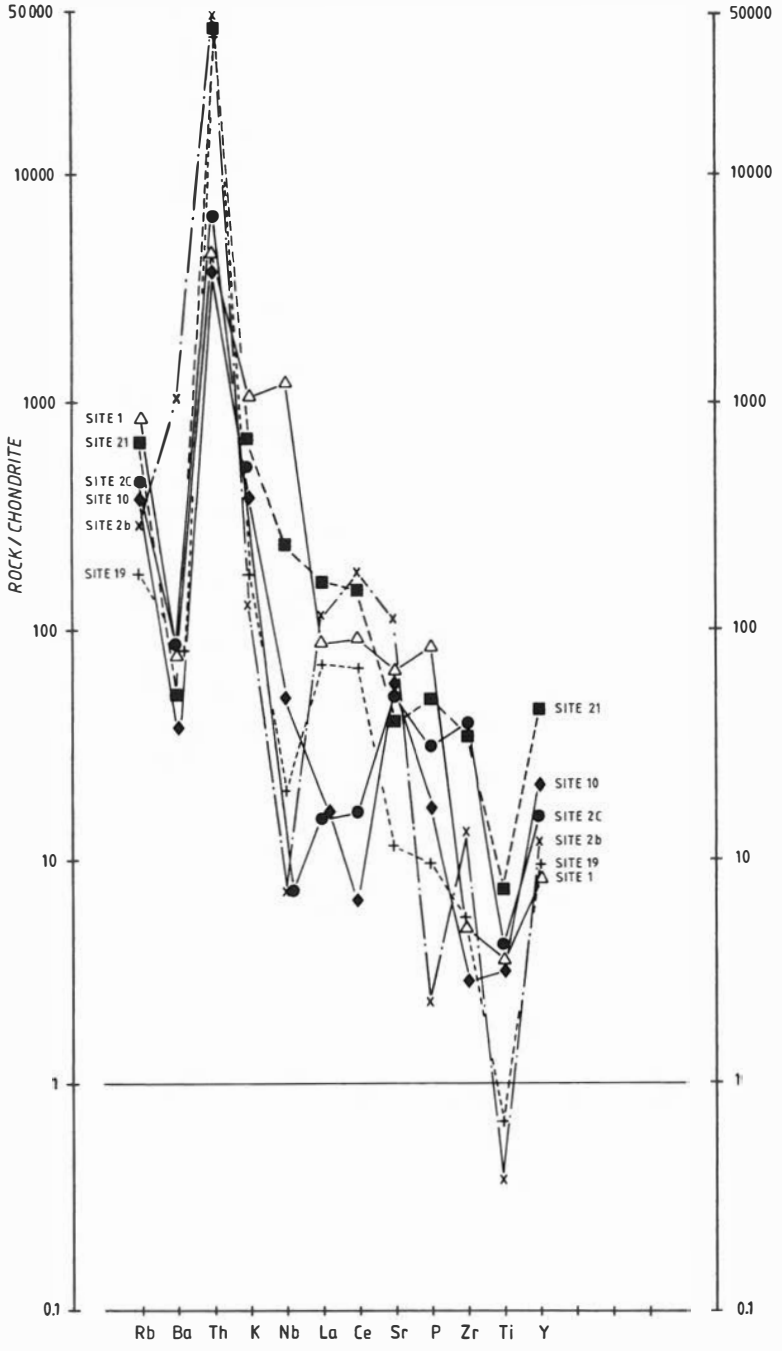

Fig. 7. Chondrite-normalized spidergram of incompatible elements for red carbonate-thorium veins. Normalizing values in ppm (Thompson et al. 1984): Rb – 0.35, Ba – 6.9, Th – 0.042, K – 120, Nb – 0.35, La – 0.328, Ce – 0.865, Sr – 11.8, P – 46, Zr – 6.84, Ti – 620, Y – 2.0.

possess a weak 'ferro-magnetism' with Neel-temperatures in the 60–120°C range, thus low-blocking components could be attributed to chemical remanent magnetization (CRM) in goethite. Associated with the later potassic fenites and TE-breccias, haematite and magnetite are common, haematite commonly occurring as minute inclusions in K-feldspar. We consider that the origin of NRM in almost all tested samples, including host-rock samples, is due to thermo-

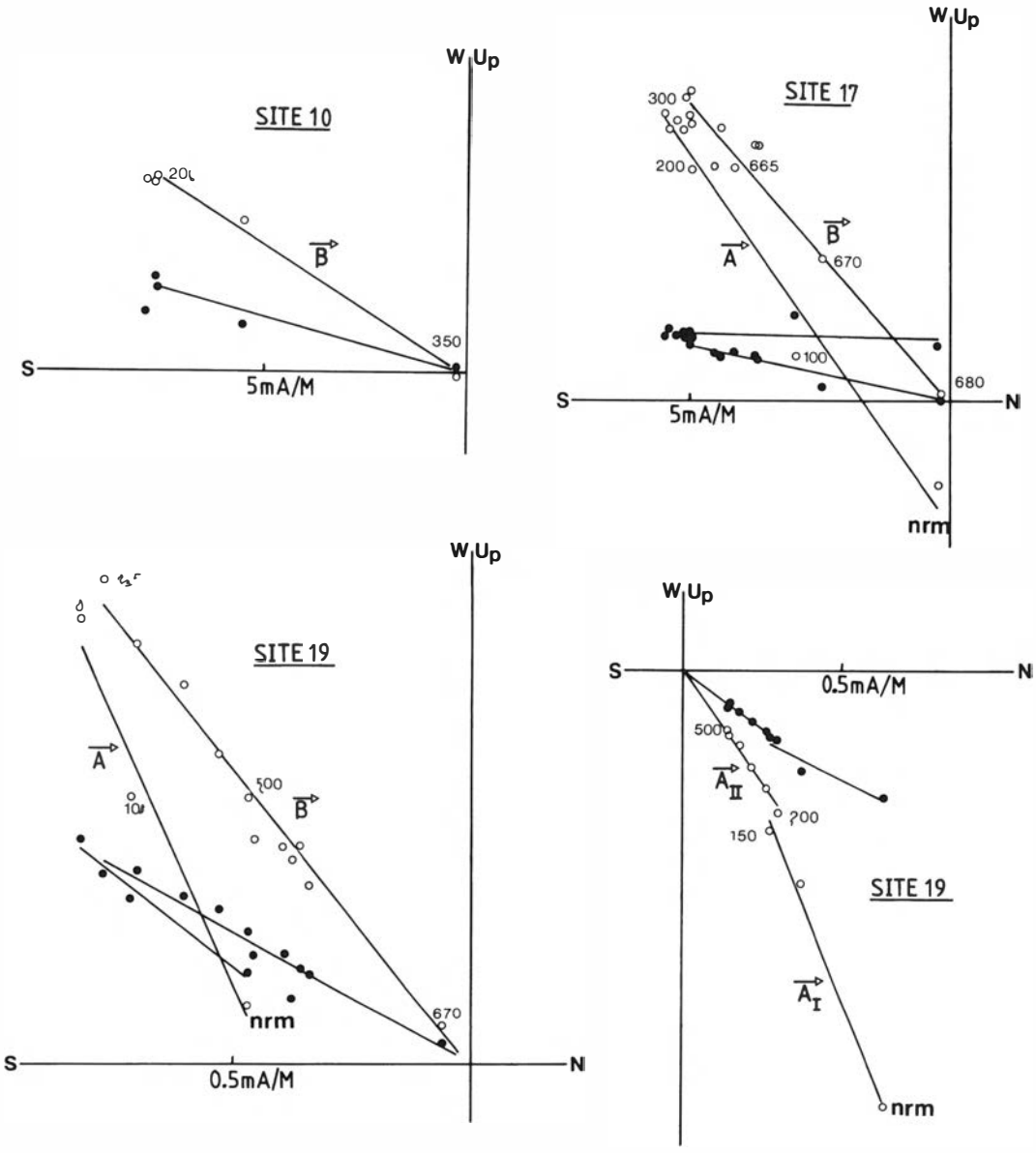

Fig. 8. Examples of thermal demagnetization of breccia samples (numbers refer to site). In vector diagrams, open and closed symbols denote points in the vertical plane.

chemical processes determined by the composition and temperature of the hydrothermal fluid(s).

Site 10 embraces a 5 m wide red alteration zone and associated carbonate-fluorite breccia (Table 2). Two remanence components, A and B, are identified. A describes northerly declinations and steeply downward dipping inclinations (normal polarity), whereas B (Fig. 8) shows southerly declinations with upward-pointing inclinations (reverse polarity). At site 10, A is exclusively identified in samples from the red breccia, whereas B is found in host-rock samples. There are no blocking temperature contrasts

Table 3. Palaeomagnetic results.

Site	Class	D°	I°	a95	N	N°	E°	dp/dm
1	AII	352	+60	35.6	3	68	207	41/54
	B	229	−36	22.8	4	36	131	15/26
10	AI	358	+71	12	7	82	199	18/21
	B	171	−38	16	3	47	204	11/19
17	AII	003	+61	9.3	9	68	185	11/14
	B	181	−32	11.5	10	44	190	7/13
19	AI	024	+71	4.3	12	76	124	7/7
	AII	039	+57	6	14	55	130	6/9
	B	211	−38	7.2	9	43	150	5/9
26A	AII	009	+51	11	3	58	177	16/23
	B	201	−33	14	2	42	164	9/16
27	AII	357	+55	17	5	62	196	17/24
Verran Fault	AI	025	+71	10.7	10	75	123	16/19
	B	196	−25	22.4	5	38	171	13/24
Hitra Fault	AI	021	+54	22.2	8	58	157	22/31
Final statistics:								
COMP.A(AI + AII)		012	+62	7.0	9*	69	167	8/11
COMP.AI		016	+71	7.5	3*	79	139	11/13
COMP.AII		010	+57	8.4	6*	63	173	9/12
COMP.B		198	−35	14.8	6*	44	167	10/17

D° = mean declination in degrees; I° = mean inclination in degrees; a95 = 95% confidence circle; N = number of samples/sites*; Pole: N° = North latitude in degrees; E° = East longitude in degrees; dp/dm = semi-axis of confidence around the mean-pole. Mean sampling co-ordinates: N 63.6, E 11.1 (Ytterøy).

between these two components, and from this site both components are associated with discrete unblocking below 350–450°C.

The remanence pattern as exemplified above is seen at most sites (Table 3, Fig. 10a), yet there are indications that A can be subdivided (AI & AII). Site 19 embraces a 30 m wide zone of hydrothermally altered and brecciated rocks, the latter located to three discrete TE-breccias (Fig. 9). When A and B are identified at sample level (Fig. 8), A always conforms to the low unblocking temperature region (<250–300°C). In the TE-breccias (A, C, D; Fig. 9), however, A predominates and is associated with blocking temperatures up to 600°C. In the latter case, A is composite, AI and AII (Figs. 8, 10b), and AI is typically erased below 200°C and is more steeply inclined than AII. These TE-breccias show high gamma-radiation, and peaks in gamma-radiation clearly correlate with the frequency of identified A components (Fig. 9). AI is exclusively located in late-stage TE-breccias.

The foregoing examples (sites 10, 19) show a bipolarity of magnetizations where A is related to red breccias and late-stage hydrothermal alteration, whilst B is often a characteristic feature of the host rock. The remaining sites do not reveal this clearcut pattern, and B is recurrently identified as a high-blocking component in red breccias (Fig. 8, site 17). B is resident in metasomatically formed haematite which occurs together with thorium minerals. The observed multi-component interplay of A and B is similar to that encountered in the Ytterøy lamprophyre dyke (Torsvik et al. 1988b). Samples from the Verran Fault Zone also show this pattern, whereas B is either absent or at least not adequately identified in the tested breccia along the Hitra–Snåsa Fault.

In order to furnish temporal constraints, a spherical cubic spline or apparent polar wander path (APWP) detailed in Torsvik et al. (1988a) is used as a 'reference'. The APWP, in the 290–255 Ma range, is constrained from Late Carboniferous and Permian poles (all reverse polarity data) with satisfactory age control. A (normal polarity) is always associated with TE-breccias and late stage hydrothermal alteration, whereas B (reverse polarity) often characterizes the host-rocks, though other red breccias also show the B component. B is most likely Permian in origin, and this oldest phase of brecciation/metasomatism appears coeval with the intrusion of the Ytterøy lamprophyre dyke (Fig. 11) (Torsvik et al. 1988b). The palaeomagnetically obtained age from this dyke corresponds well with a Rb/Sr biotite age of 256 Ma (Priem et al. 1968). A is of Mesozoic origin, but as pointed out earlier it is evident that A can have a multiple origin (AI and AII). Apart from site 19, a subdivision of the A components is not statistically straightforward. Hence, our subdivision is tentative and based on subjective pattern-recognition at site level (Fig. 10a). As for the B component, A is most likely metasomatic (thermochemical) in origin, and apart from site 19 no differences in the blocking-temperature spectra can be envisaged for AI and AII. Seen in conjunction with the APWP as outlined in Fig. 11, a Late Jurassic/Cretaceous age is indicated for AII, whereas AI gives a Tertiary age (Fig. 11). Thus, the palaeomagnetic data indicate a protracted fault-history with repeated brecciation, metasomatism and weathering, spanning from Permian to Tertiary times. A pro-

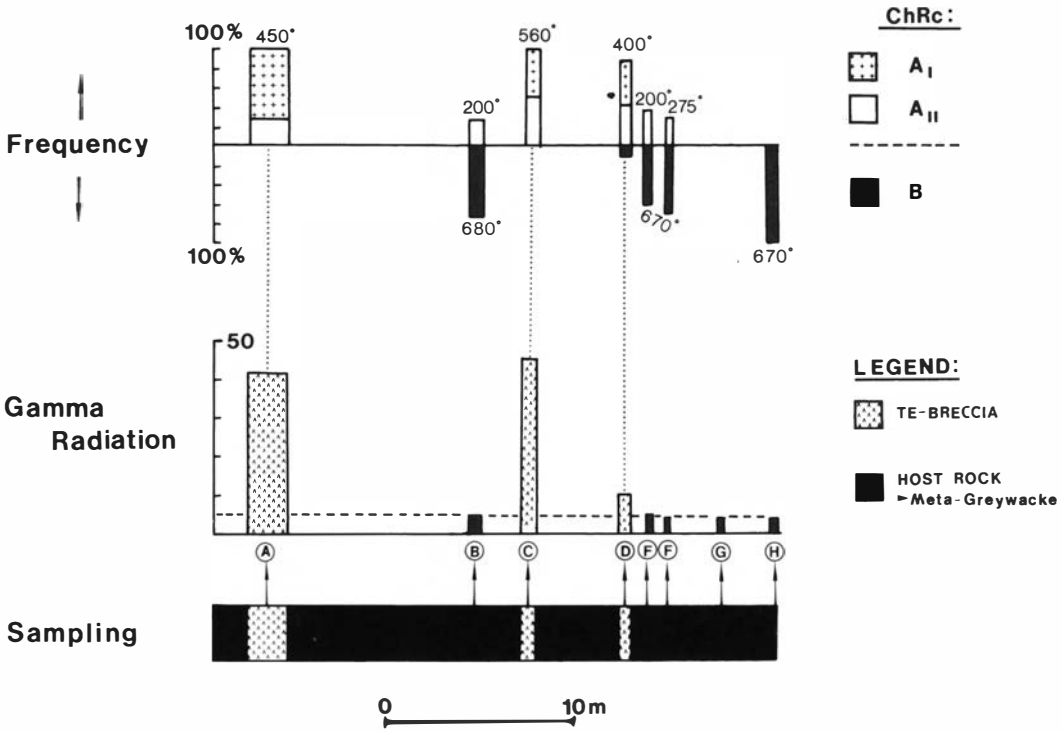

Fig. 9. Sampling locations, total gamma-radiation and the frequency of A (AI/AII) and B components from site 19. Note that A is exclusively located in the TE-breccias.

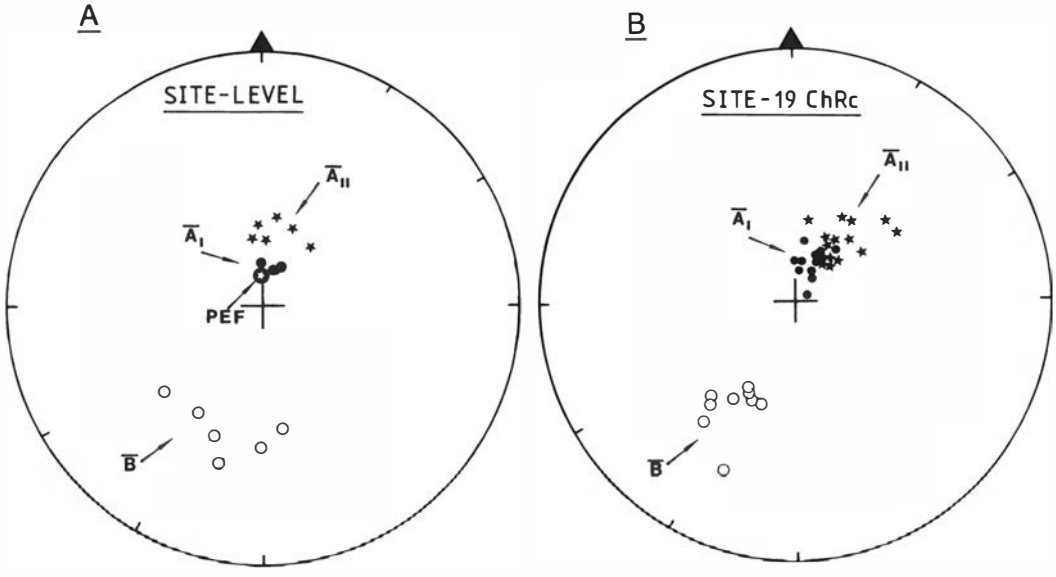

Fig. 10. Characteristic site-means from breccias and host-rocks (A), and an example of the within-site distribution (B). PEF = present day field. Cf. text.

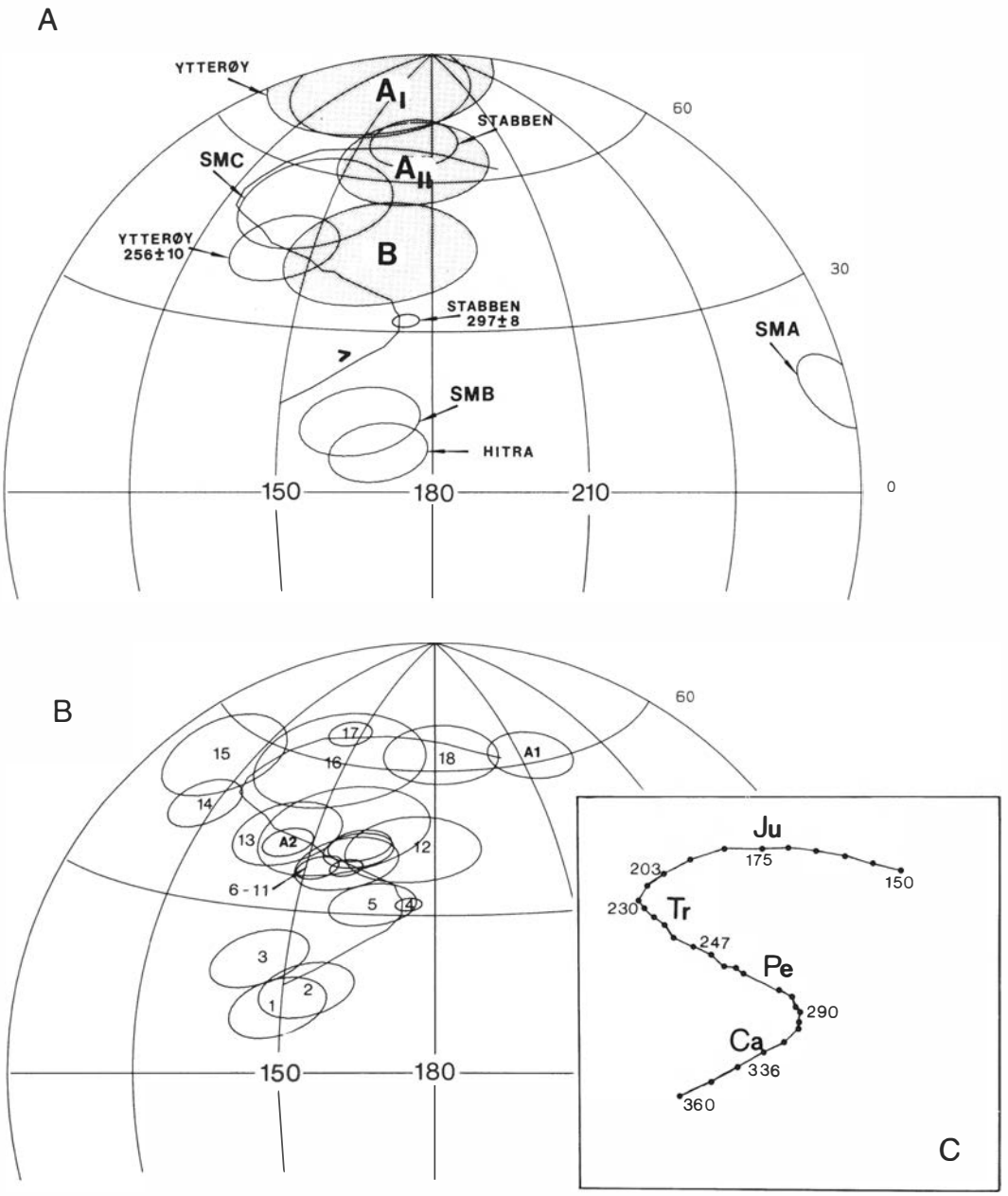

Fig. 11. (A) The relative pole-position of AI, AII and B and results from e.g. the Ytterøy lamprophyre dyke (Torsvik et al. 1988b) plotted in the frame of a spherical smoothed spline outlined in Torsvik et al. (1988a). The reported poles are plotted with shaded dp/dm semi-confidences. See Torsvik et al. (1988a) for details. (B) Palaeomagnetic poles from Norway which form the basis of the spherical smoothed spline (cf. Torsvik et al. 1988b). (C) Details in the fitted spline. Numbers denote mill. years. Ca = Carboniferous; Pe = Permian; Tr = Triassic and Ju = Jurassic.

gramme of Th-Pb and fission-track dating on fault rocks will be carried out in co-operation with the U.S.G.S. and K-Ar dating with Dr. J. Mitchell (Univ. of Newcastle) and it is hoped that a more definitive timing of events will be achieved.

Discussion

Following Le Bas (1977) we use the term fenitization referring to alkali-metasomatism in general. Le Bas argues for two principal styles of fenitization, one involving the formation of mainly sodic, together with some potassic, minerals. The other producing mainly potassic minerals. The former process is termed sodic fenitization, or just fenitization, the latter potassic fenitization or feldspathic fenitization.

In the Trondheimsfjord the only possible evidence of rift-related magmatism is the Ytterøy lamprophyre dyke (Carstens 1961), though in the western part of the MTFZ two alkali-syenite sills of Late Carboniferous age have been described (Råheim 1974; Sturt & Torsvik 1987). However, the linking of the Trondheimsfjord thorium-enriched carbonate veins with a possible alkaline and/or carbonatite intrusion must be somewhat speculative. In our view, the following arguments tend to support the hypothesis of a subcropping alkaline/carbonatite complex situated below the inner Trondheimsfjord basin.

(1) The Trondheimsfjord thorium-enriched carbonate veins resemble some of the thorium veins described from the USA, where the association with carbonatites and/or alkaline igneous rocks is well documented (see review by Staatz 1974). In particular vein-systems of the Lemhi Pass (Staatz 1972b), Wet Mountains (Christman et al. 1959; Armbrustmacher 1979, 1984) and Powderhorn district (Olson & Wallace 1956; Olson & Hedlund 1981) appear to show a similar mineralogy and mode of occurrence to those in the Trondheimsfjord. These veins, however, appear to have a higher REE/Th-ratio than the Trondheimsfjord veins which are rather low in REE. In this respect the Trondheimsfjord veins more closely resemble veins in the Hall Mountain area which have a low REE/Th-ratio (Staatz 1972a, 1974) whilst showing a higher Th-grade. In the Trondheimsfjord system all analysed samples are uniformly richer in Th than Ce + La + Y, and no systematic zonation of these elements is detectable in the present data base.

In the Powderhorn district, thorium-enriched veins occur up to 25 km away from the Iron Hill carbonatite. In other instances such veins occur in districts without exposed carbonatites or alkaline rocks, but one or both are found in 8 out of 13 vein areas (Staatz 1974). Also, Heinrich & Moore (1970), in describing feldspathic fenites in the USA and East Africa, noted that they may occur as fracture-controlled replacement veins in districts devoid of any other manifestations of alkaline igneous activity.

(2) Although alkaline magmatism is generally associated with continental rifting, the association of carbonatites, albitites, breccias and fenites with important strike-slip faults is also well documented, e.g. lamprophyre and carbonatite dike swarms along the Alpine Fault, New Zealand (Cooper 1971) and albitites and carbonatitic veins with fenitized borders near the Great Glen Fault (GGF) (Fig. 12) (Garson et al. 1984). In the latter case, the alteration products are similar to those of classical fenites around igneous carbonatite complexes. Occurrences of red-to-orange albitite-breccias, e.g. at Moniack Burn, which are stained with iron-oxides and are strongly radioactive, appear to be similar to products of early fenitization from the Trondheimsfjord area. Along the GGF there is, at present, no evidence of later-stage hydrothermal activity such as potassium-metasomatism or formation of TE-breccias. The GGF-fenites are believed to have formed during the emplacement of at least one carbonatite mass into the fault zone, possibly during a period of Early Devonian extensional faulting.

(3) Intense alkali-metasomatism is a characteristic feature associated with carbonatites (Le Bas 1981). In the Trondheimsfjord area both sodic and potassic metasomatism of the host-rocks is apparent, the latter being dominant. Early metasomatism led to replacement of the host-rock by such minerals as albite, quartz and apatite. It is, however, doubtful that the early metasomatism can be referred to as fenitization since peralkaline minerals like aegirine and arfvedsonite have not been identified.

The most important stage of alkali-metasomatism corresponds to the K-feldspar/Th-hydrothermal phase, locally leading to the alter-

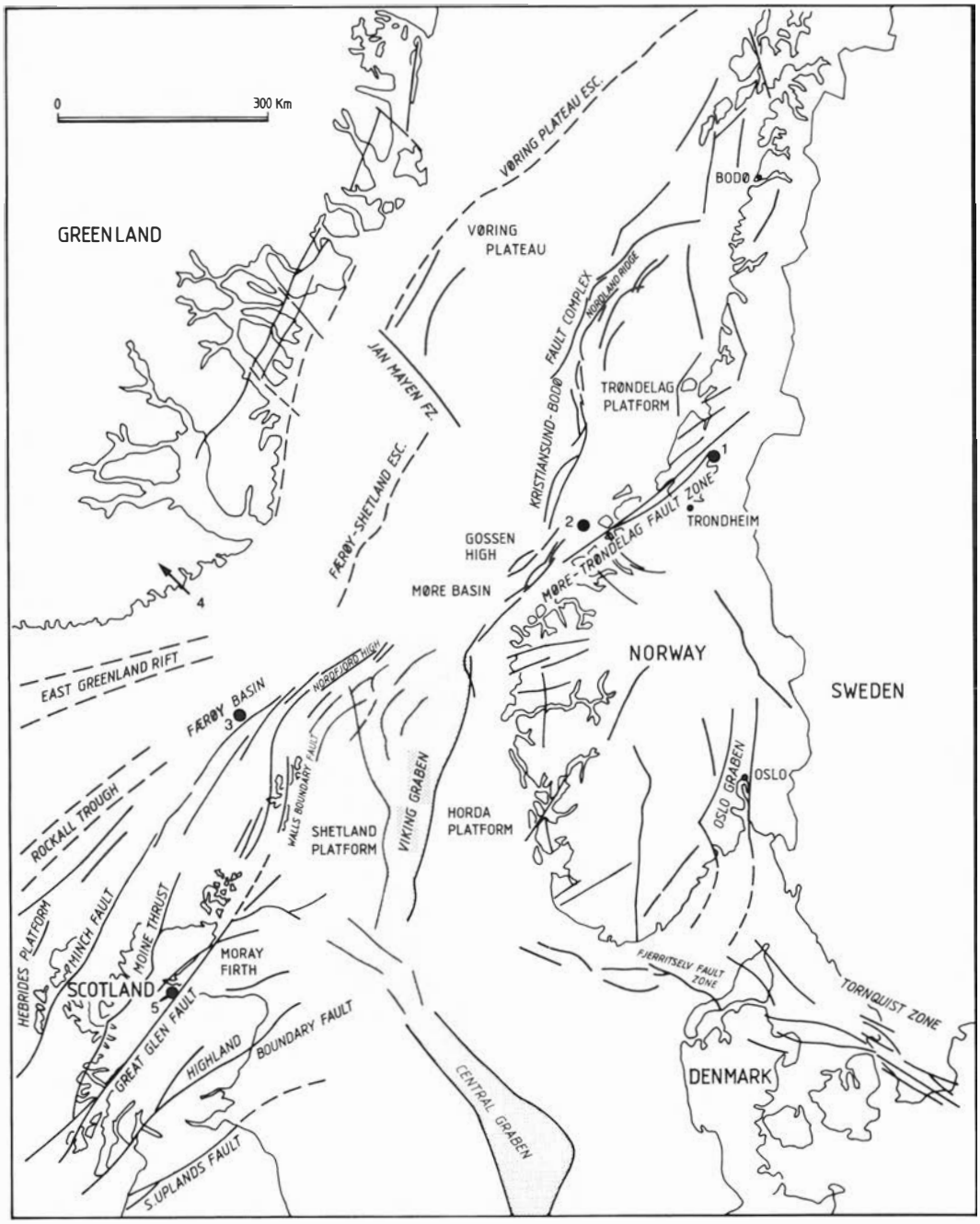

Fig. 12. Map showing some of the major tectonic structural features of the northern North Sea and Norwegian Sea, and principal onland faults in Scotland and Norway. (1) Location of red thorium-enriched carbonate veins along the Møre–Trøndelag Fault Zone. (2) Position of the Palaeocene/Eocene Vestbrona olivine–nephelinite volcanic rocks (Bugge et al. 1980). (3) The Palaeocene/Eocene Færøy–Shetland intrusive belt (Hitchen & Ritchie 1987). (4) The Tertiary East Greenland alkaline rock province. For details, see Nielsen (1987). (5) Area affected by fenitization along the Great Glen Fault (Garson et al. 1984). Map modified from Færseth (1984).

ation of the original host-rocks to a feldspathic fenite (Sutherland 1965; Heinrich & Moore 1970; Le Bas 1981) mainly composed of microcline or adularia. As described by Heinrich & Moore 1970) this potassic metasomatism is typical of many alkaline/carbonatitic complexes occurring in the USA and Africa and clearly postdates the Na-metasomatism.

According to Rubie & Gunter (1983), the factors that determine partitioning of Na-K between feldspar and fluid, and which determine the fenite type, include temperature, pressure, and the CO_2 content of the fluid. Thus, spatial and temporal variations in fenitization products must be expected around carbonatites. The development of sodic fenite at deep crustal levels and potassic fenite at shallower levels near an intrusion can be related to temperature gradients in the thermal aureole (cf. Le Bas 1981). This implies that the exposed Trondheimsfjord veins may belong to the outer zone of carbonatite activity.

Apart from showing a dominant potassic fenitization and late-stage residual mineralization, the Trondheimsfjord vein system also shows a high Th/U-ratio (28/1), which is another characteristic of carbonatites (Le Bas 1977).

(4) Concerning the timing of the main rifting stages in the Trondheimsfjord system, the palaeomagnetic data indicate three main stages of rifting, magmatic and/or hydrothermal activity. The first phase occurred during Permian times with intrusion of the Ytterøy lamprophyre dyke and the onset of early hydrothermal activity represented by Na-metasomatism and later replacement by iron-carbonate minerals and K-feldspar. Permian alkaline activity is well documented from Western Norway (Færseth et al. 1976) and from the Oslo Graben (Ramberg & Larsen 1978). Alkaline dyke swarms occurring in the Northern parts of the British Isles have been assigned a Late Carboniferous/Early Permian age associated with the developing Variscan orogeny to the south (Russell & Smythe 1983).

A later phase of rifting, corresponding with the formation of TE-breccias, probably occurred in Late Jurassic/Early Cretaceous times. The main faulting activity in on-land MTFZ was then apparently confined to the Verran Fault (Fig. 1) (Grønlie & Roberts 1987, and in prep.), forming a dextral strike-slip duplex system. Locally, in the Trondheimsfjord area, dextral movement on the Mosvik splay fault (Fig. 1) led to an extensional regime favouring hydrothermal activity along faults and joints.

The latest hydrothermal activity in the Trondheimsfjord system occurred even later as quartz, calcite and fluorite were deposited in open joints. Fission-track dating of fluorite (blocking temp. approx. 108°C) provides an upper limit for the timing of the latest hydrothermal activity i.e. Late Cretaceous/Early Tertiary times (V. Harder pers. comm.). This latest hydrothermal event was presumably related to the tectonic events which led to the Eocene opening of the Norwegian–Greenland Sea (Talwani & Eldholm 1977). At this time alkaline volcanism flanking the initial North Atlantic rift occurred both in East Greenland (Nielsen 1987) and in Norway, at Vestbrona, within the MTFZ (Bugge et al. 1980) (Fig. 12). In the Færøy–Shetland Basin a major phase of Palaeocene–Early Eocene igneous activity related to the opening of the North Atlantic occurred (Hitchen & Ritchie 1987).

Conclusions

It is proposed that the red thorium-enriched carbonate veins, occurring around the inner Trondheimsfjord basin, may be products of fenitization related to a subcropping carbonatite intrusion. The mineral parageneses and metasomatic products along fault-related alteration zones in the Trondheimsfjord basin bear many similarities to those that can be related to hydrothermal activity associated with carbonatite intrusions.

Host-rocks were altered by an early phase of sodic metasomatism, followed by invading Fe, Mg and CO_2-rich fluids. The main stage of alkali-metasomatism was a later pervasive potassic alteration rich in Th and Fe. Later stage hydrothermal activity is evidenced by fluorite, quartz and calcite veins.

The investigated area is situated centrally within the long-lived Møre–Trøndelag Fault Zone (MTFZ). This fault zone was probably initiated in mid-Palaeozoic time, and important phases of movement have been postulated during Late Devonian, Permian and Late Jurassic/Early Cretaceous time. The red iron-carbonate veins correspond to a Permian phase of tectonic activity attendant on the formation of breccias and hydrothermal alteration. These are cut by TE-breccias, which we relate to a local extensional regime

developed in association with Late Jurassic/Early Cretaceous dextral strike-slip movement on the Verran Fault. The palaeomagnetic data and fission-track dating of fluorite indicates that the latest hydrothermal event within the Trondheimsfjord fault system was at latest of Late Cretaceous/ Early Tertiary age, i.e. just prior to the opening of the Norwegian–Greenland Sea.

Acknowledgements. – The authors are grateful to Statoil and the Norwegian Research Council for Science and the Humanities (Grant no. D.41.12.021) for financial support. We also acknowledge Ron Boyd, Peter Ihlen and Jan Sverre Sandstad for comments on an early version of the manuscript, and discussion with Don Tarling and Brian Sturt. Improvements of the manuscript by Tom Andersen and an anonymous reviewer are greatly appreciated. The figures were drawn by Gunnar Grønli. Jomar Staw and Ole Sivert Hembre are thanked for participation in the field.

Norwegian Lithosphere Contribution no. 45.

Manuscript received June 1988

References

Armbrustmacher, T. J. 1979: Replacement and primary magmatic carbonatites from the Wet Mountains area, Fremont and Custer Counties, Colorado. *Economic Geology 74*, 888–901.

Armbrustmacher, T. J. 1984: Alkaline rock complexes in the Wet Mountains area, Custer and Fremont Counties, Colorado. *United States Geological Survey Professional Paper 1269*, 33 pp.

Bugge, T., Prestvik, T. & Rokoengen, K. 1980: Lower Tertiary volcanic rocks off Kristiansund – Mid Norway. *Marine Geology 35*, 277–286.

Carstens, H. 1961: A post-Caledonian ultrabasic lamprophyre dyke on the island of Ytterøy in the Trondheimsfjord, Norway. *Norsk Geologisk Tidsskrift 47*, 10–21.

Christman, R. A., Brock, M. R., Pearson, R. C. & Singewald, Q. D. 1959: Geology and thorium deposits of the Wet Mountains, Colorado. A progress report. *United States Geological Survey Bulletin 1072-H*, 491–533.

Cooper, A. F. 1971: Carbonatites and fenitization associated with a lamprophyric dike-swarm intrusive into schists of the New Zealand geosyncline. *Geological Society of America Bulletin 82*, 1327–1340.

Færseth, R. B., MacIntyre, R. M. & Naterstad, J. 1976: Mesozoic alkaline dykes in the Sunnhordland region, western Norway: ages, geochemistry and regional significance. *Lithos 9*, 331–345.

Færseth, R. B. 1984: Tectonic map of the Northeast Atlantic. Norsk Hydro.

Gabrielsen, R. H. & Ramberg, I. B. 1979: Fracture patterns in Norway from Landsat imagery: results and potential use. *Proceedings Norwegian Sea Symposium, Tromsø, NSS/23*, 1–28.

Garson, M. S., Coats, J. S., Rock, N. M. S. & Deans, T. 1984: Fenites, breccia dykes, albitites, and carbonatitic veins near the Great Glen Fault, Inverness, Scotland. *Journal of the Geological Society London 141*, 711–732.

Grønlie, A. 1984: Naturlig radioaktiv stråling fra berggrunnen i Nord–Trøndelag fylke. *Norges geologiske undersøkelse rapport 84.100*, 10 pp.

Grønlie, A. & Roberts, D. 1987: Dextral strike-slip duplexes of Mesozoic age along the Hitra–Snåsa and Verran Faults, Møre–Trøndelag Fault Zone, Central Norway. *Norges geologiske undersøkelse rapport 87.139*, 24 pp.

Grønlie, A. & Roberts, D. 1989: Resurgent strike-slip duplex development along the Hitra–Snåsa and Verran Faults, Møre–Trøndelag Fault Zone, central Norway. *Journal of Structural Geology* 11 (in press).

Grønlie, A. & Staw, J. 1987: Oppfølging av naturlige strålingsanomalier i Nord-Trøndelag med Fosen. *Norges geologiske undersøkelse rapport 87.053*, 31 pp.

Heinrich, E. W. & Moore, D. G. 1970: Metasomatic potash feldspar rocks associated with igneous alkalic complexes. *Canadian Mineralogist 10*, 571–598.

Hitchen, K. & Ritchie, J. D. 1987: Geological review of the West Shetland area. *In* Brooks, J. & Glennie, K. (eds.): *Petroleum Geology of North West Europe*, Graham & Trotman, 737–749.

Kjerulf, T. 1875: *Om Trondhjems Stifts geologi.* Johan Dahl, Christiania.

Larsen, V. B. 1987: A synthesis of tectonically-related stratigraphy in the North Atlantic-Arctic region from Aalenian to Cenomanian time. *Norsk Geologisk Tidsskrift 67*, 281–293.

Le Bas, M. J. 1977: *Carbonatite-Nephelinite Volcanism. An African Case History.* John Wiley & Sons, 347 pp.

Le Bas, M. J. 1981: Carbonatite magmas. *Mineralogical Magazine 44*, 133–140.

Mitchell, J. G. & Roberts, D. 1986: Ages of lamprophyre dykes from Ytterøy and Lerkehaug, near Steinkjer, Central Norwegian Caledonides. *Norsk Geologisk Tidsskrift 66*, 255–261.

Nielsen, T. F. D. 1987: Tertiary alkaline magmatism in East Greenland: a review. *In* Fitton. J. G. & Upton, B. G. J. (eds.): *Alkaline Igneous Rocks. Geological Society Special Publication 30*, 489–515.

Olson, J. C. & Wallace, S. R. 1956: Thorium and rare-earth minerals in the Powderhorn District, Gunnison County, Colorado. *United States Geological Survey Bulletin 1027-O*, 693–721.

Olson, J. C. & Hedlund, D. C. 1981: Alkalic rocks and resources of thorium and associated elements in the Powderhorn District, Gunnison County, Colorado. *United States Geological Survey Professional Paper 1049-C*, 34 pp.

Priem, H. N. A., Verschure, R. H., Boelrijk, N. A. I. M. & Hebeda, E. H. 1968: Rb-Sr and K-Ar age measurements of phlogopitic biotite from the ultrabasic lamprophyre dyke on the island of Ytterøy, Trondheimsfjord, Norway. *Norsk Geologisk Tidsskrift 48*, 319–321.

Ramberg, I. B. & Larsen, B. T. 1976: Tectonomagmatic evolution. *In* Dons, J. A. & Larsen, B. T. (eds.): *The Oslo Paleorift. Norges Geologiske Undersøkelse Bulletin 337*, 55–73.

Rubie, D. C. & Gunter, W. D. 1983: The role of speciation in alkaline igneous fluids during fenite metasomatism. *Contributions to Mineralogy and Petrology 82*, 165–175.

Russell, M. J. & Smythe, D. K. 1983: Origin of the Oslo Graben in relation to the Hercynian-Alleghenian orogeny and lithospheric rifting in the North Atlantic. *Tectonophysics 94*, 457–472.

Råheim, A. 1974: A post-Caledonian syenite porphyry dyke in the Western Gneiss region, Tustna, Central Norway. *Norsk Geologisk Tidsskrift 54*, 139–147.

Staatz, M. H. 1972a: Thorium-rich veins of Hall Mountain northernmost Idaho. *Economic Geology 67*, 240–248.

Staatz, M. H. 1972b: Geology and description of the thorium-bearing veins, Lemhi Pass quadrangle, Idaho and Montana. *United States Geological Survey Bulletin 1351*, 94 pp.

Staatz, M. H. 1974: Thorium veins in the United States. *Economic Geology 69*, 494–507.

Staatz, M. H. 1983: Geology and description of thorium and rare-earth deposits in the southern Bear Lodge Mountains, northeastern Wyoming. Geology and resources of thorium in the United States. *United States Geological Survey Professional Paper 1049-D*, 52 pp.

Staw, J. 1986: Registrering av hydrotermale soner i Nord-Trøndelag. *Norges geologiske undersøkelse rapport 86.052*, 13 pp.

Sturt, B. A. & Torsvik, T. H. 1987: A late Carboniferous palaeomagnetic pole recorded from a syenite sill, Stabben, Central Norway. *Physics of the Earth and Planetary Interiors 49*, 350–359.

Sturt, B. A., Torsvik, T. H. & Grønlie, A. 1987: Dating of hydrothermal alteration-zones and breccias in the Trondheimsfjord region: The Møre–Trøndelag Fault Zone. *Norges geologiske undersøkelse rapport 87.138*, 11 pp.

Sutherland, D. S. 1965: Nomenclature of the potassic-feldspathic rocks associated with carbonatites. *Geological Society of America Bulletin 76*, 1409–1412.

Talwani, M. & Eldholm, O. 1977: Evolution of the Norwegian–Greenland Sea. *Geological Society of America Bulletin 88*, 969–999.

Thompson, R. N., Morrison, M. A., Hendry, G. L. & Parry, S. J. 1984: An assessment of the relative roles of crust and mantle in magma genesis: an elemental approach. *Phil. Trans. R. Soc. Lond. A 310*, 549–590.

Torsvik, T. H., Sturt, B. A., Ramsay, D. M., Grønlie, A., Roberts, D., Smethurst, M., Atakan, K., Bøe, R. & Walderhaug, H. J. 1988a: Palaeomagnetic constraints on the early history of the Møre–Trøndelag Fault Zone, Central Norway. *In* Laj, C. & Kissel, C. (eds.): *Palaeomagnetic Rotations and Continental Deformation.* Reidel (in press).

Torsvik, T. H., Sturt, B. A., Grønlie, A. & Ramsay, D. M. 1988b: Palaeomagnetic data bearing on the age of the Ytterøy dyke, Central Norway. *Physics of the Earth and Planetary Interiors* (in press).

Wolff, F. C. 1976: *Geologisk kart over Norge, berggrunnskart Trondheim 1:250,000.* Norges Geologiske Undersøkelse.

Wolff, F. C. 1984: Regional geophysics of the Central Norwegian Caledonides. *Norges geologiske undersøkelse bulletin 397*, 1–27.